Effects of Gradient Amplitude and Duration on Q-Space Imaging

H. H. Ong[1], A. C. Wright[1], S. L. Wehrli[2], A. Souza[1], E. D. Schwartz[1], P. K. Saha[1], and F. W. Wehrli[1]

[1]Laboratory for Structural NMR Imaging, Department of Radiology, University of Pennsylvania School of Medicine, Philadelphia, Pennsylvania, United States, [2]NMR Core Facility, Children's Hospital of Philadelphia, Philadelphia, Pennsylvania, United States

Introduction

Q-space imaging[1] (QSI) offers potential for indirect of assessment of microarchitecture by exploiting the regularity of restrictions to molecular diffusion in porous systems as previously applied to white matter (WM) axonal architecture[2,3]. The Fourier transform (FT) of the QSI echo attenuation is known as the displacement profile (DP), and contains pore geometry information. However, this FT relationship only applies in the short pulse gradient approximation (SPGA) ($\delta << D$, where δ and Δ are the gradient duration and diffusion time). Violation of the SPGA leads to artificial DP narrowing[2,4]. Furthermore, q_{max} ($q = (2\pi)^{-1}\gamma\delta\mathbf{G}$ where γ and $\mathbf{G}$ are the gyromagnetic ratio and gradient amplitude) determines DP resolution ($\Delta r = (2q_{max})^{-1}$). The need for high DP resolution to study WM and imposition of the SPGA demands very high gradient amplitudes not commercially available. Previous work consequently either violated the SGPA or their DP resolutions exceeded typical axon diameters. Using a home-built high-amplitude gradient set[5], we are able to generate high DP-resolution DP maps that can differentiate WM tracts of mouse spinal cords (SP)[6]. Here we report experimental data showing the consequences of both low DP resolution and violating the SPGA. By first acquiring a DP map of a mouse SP under nearly ideal conditions, we can compare the data with DP maps of low resolution and results from experiments violating the SPGA.

Method

Five SP cervical sections were dissected from perfusion-fixated 8-10 month-old female C57 BL/6 mice. To obtain high DP resolution, experiments were performed with a custom-built 50 T/m z-gradient coil in conjunction with a solenoidal RF coil (4-turn, 3*mm* i.d.) set interfaced to a 9.4 T spectrometer/micro-imaging system (Bruker DMX 400 with Micro2.5 gradients and BAFPA40 amplifiers). A diffusion-weighted stimulated-echo sequence was used: 64x64, sw=25kHz, TR=2s, Δ/δ=10/0.4 *ms*, FOV/THK=4/1*mm*, and an ambient temperature of 19 °C. The diffusion gradient was applied along the z-axis (perpendicular to SP long axis) in 64 increments of q (q_{max}=0.82 μm^{-1}, Δx=0.6μm) and zero-filled to 128 q-values. A q-space attenuation plot was obtained for each pixel and Fourier transformed to produce the DP. FWHM, kurtosis, and zero-displacement probability values were then from the DP and assigned to that pixel location. ROIs (10-20 pixels, after zero-filling) were selected within the cuneatus (FC), gracilis (FG), and dorsal corticospinal (dCST) tracts (mean axon diameter: dCST<FG<FC). All image processing was performed in IDL. This protocol will be repeated with Δ/δ=10/5 *ms* in order to simulate conditions violating the SPGA. To simulate reduced DP resolution, the q-space data above was truncated at $q=q_{max}/4$, zero-filled to 128 points and processed as above. One cervical section was stained for myelin (toluidine blue) and optical microscopic images were obtained for the cuneatus, gracilis, and dCST regions. The images were then manually segmented into ECF, ICF and myelin regions, and mean axon diameters calculated by equating the ICF area of each axon to a circle.

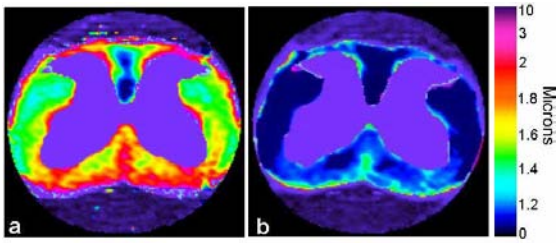

Fig. 1 DP FWHM maps for a single specimen derived from long δ (a) and short δ acquisitions (b). Diffusion sensitization was perpendicular to SP axis (vertical image axis).

Results and Discussion

Fig. 1 shows DP FWHM maps derived from long and short δ acquisitions (without q-space truncation) for one specimen and Fig. 2 shows the corresponding q-space echo attenuations. Note the smaller displacements and reduced attenuation in the long-δ DP map and q-space plot, respectively. Due to space limitations, Table 1 compares only DP FWHMs at short and long δ experiments and with and without q-space truncation averaged across 5 specimens. Kurtosis and zero displacement probability values showed similar behavior. Within a ROI, mean DP FWHM, kurtosis and zero-displacement probability values correlated well with the histologic mean axon diameters (data not shown). Paired t-tests were run between mean DP FWHM, kurtosis and zero-displacement probability values for various WM tracts (N=5) (FC vs FG, dCST vs FC, and FG vs dCST). In the untruncated data for the short-δ case, each ROI parameter was significantly different from the others ($p<0.01$). In the long-δ experiments, with exception of zero-displacement probability, the ROI parameters were still significantly different from the others ($p<0.05$). Even with the truncated data with a lower DP resolution (Δx=2.4μm), significant differences were observed for short-δ ($p<0.05$). At long-δ, the truncated data with the same lower DP resolution also showed significant differences ($p<0.05$), with the exception of the dCST vs FG comparison. It should be noted that while DP FWHM correlates with axon diameter, further investigation is needed to understand the exact relationship between FWHM and microarchitecture.

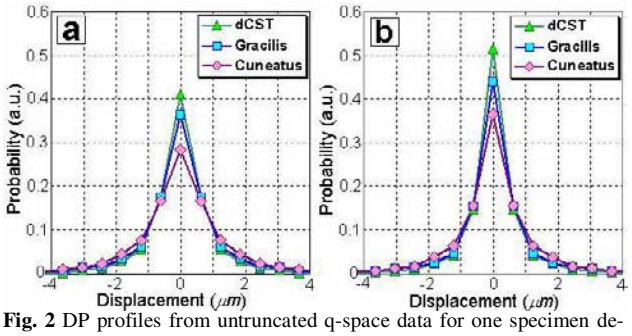

Fig. 2 DP profiles from untruncated q-space data for one specimen derived from (a) short-δ and (b) long-δ acquisitions.

Table 1. Comparing Displacement Profile FWHMs

Region	Histologic Mean Axon diameter (μm)	DP FWHM (μm) Short δ, Full q	DP FWHM (μm) Long δ, Full q	DP FWHM (μm) Short δ, 1/4 q	DP FWHM (μm) Long δ, 1/4 q
FC	1.63	1.60 ± 0.12 ($p<0.01$)*	1.06 ± 0.04 ($p<0.01$)*	3.53 ± 0.12 ($p<0.01$)*	3.34 ± 0.10 (*ns*)*
FG	1.07	1.26 ± 0.06 ($p<0.001$)$^{+}$	0.95 ± 0.06 ($p<0.01$)$^{+}$	3.37 ± 0.05 ($p<0.05$)$^{+}$	3.21 ± 0.04 ($p<0.05$)$^{+}$
dCST	0.78	1.10 ± 0.05 ($p<0.001$)$^{\#}$	0.87 ± 0.06 ($p<0.0001$)$^{\#}$	3.31 ± 0.06 ($p<0.01$)$^{\#}$	3.16 ± 0.07 ($p<0.01$)$^{\#}$

Paired t-test p-values: (*) = FC vs FG; ($^{+}$) = FG vs dCST; ($^{\#}$) = FC vs dCST;

Conclusion

For *in vivo* applications, where gradient hardware limitations are the greatest, the consequences of violating the SPGA and low DP resolution on QSI must be investigated. This work demonstrates the feasibility of low DP-resolution QSI DP maps of mouse SP to distinguish WM tracts differing in mean axon diameters while violating the SPGA.

References: 1. Callaghan, PT, *Principles of NMR Microscopy*, Oxford University Press (1991). 2. Assaf Y, *et al*, *MRM*, **47**:115-126 (2002). 3. Chin CL, *et al*, *MRM*, **52**:733-740 (2004). 4. Mitra ,*et al*, *JMR A*, **113**:94-101 (1995). 5. Wright AC, *et al*, Proc. ISMRM 12th Scientific Meeting, Kyoto, Japan, 2004, p. 741. 6. Ong H, *et al*, Proc. ISMRM 14th Scientific Meeting, Seattle, USA 2006, p. 640. **Acknowledgements:** NIH grant R21 EB003951